Structure and function analysis of a potent human neutralizing antibody CA521^{LALA} against SARS-CoV-2

Changlin Dou (douchanglin@luye.com)
Shandong Boan Biotechnology Co., Ltd.
Cheng-Feng Qin (chenfeng_qin@126.com)
Institute of Microbiology and Epidemiology, Academy of Military Medical Sciences
Lan Wang (wanglan@nifdc.org.cn)
Institute for Biological Product Control, National Institutes for Food and Drug Control (NIFDC)
Deyong Song
Shandong Boan Biotechnology Co., Ltd.
Yong-Qiang Deng
Institute of Microbiology and Epidemiology, Academy of Military Medical Sciences
Wenbo Wang
Institute for Biological Product Control, National Institutes for Food and Drug Control (NIFDC)
Chuangchuang Dong
Shandong Boan Biotechnology Co., Ltd.
Zhenfei Ning
Shandong Boan Biotechnology Co., Ltd.
Xiu Liu
Shandong Boan Biotechnology Co., Ltd.
Chuan Liu
Shuimu BioSciences Ltd.
Guangying Du
State Key Laboratory of Long-acting and Targeting Drug Delivery System, Shandong Luye Pharmaceutical Co. Ltd
Chunjie Sha
State Key Laboratory of Long-acting and Targeting Drug Delivery System, Shandong Luye Pharmaceutical Co. Ltd
Kailin Wang
Shandong Boan Biotechnology Co., Ltd.
Jun Lu
Shandong Boan Biotechnology Co., Ltd.
Baiping Sun

Shandong Boan Biotechnology Co., Ltd.

Yanyan Zhao

Shandong Boan Biotechnology Co., Ltd.

Qiaoping Wang

Shandong Boan Biotechnology Co., Ltd.

Hongguang Xu

Shandong Boan Biotechnology Co., Ltd.

Ying Li

Shandong Boan Biotechnology Co., Ltd.

Zhenduo Shen

Shandong Boan Biotechnology Co., Ltd.

Jie Jiao

Shandong Boan Biotechnology Co., Ltd.

Ruiying Wang

State Key Laboratory of Long-acting and Targeting Drug Delivery System, Shandong Luye Pharmaceutical Co. Ltd

Jingwei Tian

State Key Laboratory of Long-acting and Targeting Drug Delivery System, Shandong Luye Pharmaceutical Co. Ltd

Wanhui Liu

State Key Laboratory of Long-acting and Targeting Drug Delivery System, Shandong Luye Pharmaceutical Co. Ltd

---

Research Article

Keywords: SARS-CoV-2,neutralizing antibody,COVID-19,Structure

Posted Date: January 9th, 2021

DOI: https://doi.org/10.21203/rs.3.rs-141793/v1

Abstract

Severe acute respiratory syndrome coronavirus 2 (SARS-CoV-2) is the causative agent of the ongoing coronavirus disease 2019 (COVID-19) pandemic, which has resulted in ~1,119,431 deaths. There is currently no approved vaccines or therapeutics for treating COVID-19. The SARS-CoV-2 Spike protein promotes entry into host cells and is considered a key therapeutic target by many researchers. Here we describe the identification of several monoclonal antibodies that target the SARS-CoV-2 Spike protein. One human antibody, $CA521^{LALA}$, demonstrated neutralization potential by immunizing human antibody transgenic mice. $CA521^{LALA}$ showed potent SARS-CoV-2-specific neutralization activity against SARS-CoV-2 pseudovirus and authentic SARS-CoV-2 infection *in vitro*. The LALA mutation introduced to CA521 abrogates the binding with Fc receptors or complement receptors reducing antibody-dependent enhancement seen with anti-SARS-CoV antibodies. $CA521^{LALA}$ also demonstrated having a long half-life of 9.5 days in mice and 9.3 days in rhesus monkeys. $CA521^{LALA}$ inhibited SARS-CoV-2 infection in SARS-CoV-2 susceptible mice at a therapeutic setting with the virus titer of the lung reduced by 4.5 logs. Structural analysis by cryo-EM revealed that $CA521^{LALA}$ recognizes an epitope overlapping with angiotensin converting enzyme 2 (ACE2)-binding sites in SARS-CoV-2 receptor binding domain (RBD) in the Spike protein. $CA521^{LALA}$ blocks the interaction by binding all three RBDs of one SARS CoV-2 spike trimer simultaneously. These results demonstrate the importance for antibody-based therapeutic interventions in the treatment of COVID-19 and identifies $CA521^{LALA}$ a promising antibody that reacts with SARS-CoV-2 Spike protein to strongly neutralize its activity.

Introduction

World Health Organization as of October 21th has reported that the coronavirus disease 2019 (COVID-19) caused by the virus severe acute respiratory syndrome coronavirus 2 (SARS-CoV-2) has caused 1,119,431 deaths globally (https://www.who.int/). SARS-CoV-2 is closely related severe acute respiratory syndrome coronavirus (SARS-CoV) and belongs to the lineage B of the genus *Betacoronavirus* in the *Coronaviridae* family. There are no vaccines approved for the treatment of COVID-19. Monoclonal antibodies (MAbs) are promising candidates to combat emerging viruses. For example, in the case of Ebola virus, MAbs MAb114 and REGN-EB3 have shown striking treatment benefits, reducing the mortality rate from ~67% to 33.5- 35.1% for all patients and to 9.9-11.2% for patients with low viral loads [1]. MAbs are also being considered as promising therapeutics for COVID-19 patients [2].

Sharing an amino acid sequence identity of ~80% in the envelope-located spike glycoprotein (Sike protein), both SARS-CoV-2 and SARS-CoV use human angiotensin-converting enzyme 2 (hACE2) to enter host cells. Cellular entry is achieved by the homotrimeric S-mediated virus-receptor engagement through the receptor-binding domain (RBD) followed by virus-host membrane fusion[3, 4, 5, 6, 7]. The Spike protein is a viral factor that mediates attachment to cells and fusion of the viral and cellular membrane, functions associated with the S1 and S2 subunits respectively [3, 4, 5, 6, 7]. The primary amino acid sequence of the S1 subunit of coronaviruses determine host receptors. The structure and function of the SARS CoV-2 Spike

protein has been determined [8]. S protein trimer of coronavirus S structures always have some RBDs in an "up" conformation and some in the "down" conformation[9, 10, 11, 12]. 3D structures of SARS-CoV-2 S protein also reveal some RBDs in "up" conformations and some in the "down" conformation [8, 13, 14, 15]. The crystal structure of the RBD of the spike protein of SARS-CoV-2 bound to the cell receptor ACE2 has also been determined. This structural analysis identified the residues of the RBD that are essential for ACE2 binding [16].

Potent neutralizing antibodies including S230, m396, 80R, CR3022 have been shown to target the SARS-CoV RBD in S1, disabling receptor interactions. Unfortunately, none demonstrate potent neutralizing activity against SARS-CoV-2[12, 14, 17, 18, 19, 20]. Additionally, previous studies have shown that pre-existing serum antibodies associate with poor outcomes in patients with the 2009 influenza infection or SARS-CoV infection[21, 22, 23]. This may be due in part to antibody-dependent enhancement (ADE) which could lead to acute respiratory injury and is a potential risk for antibody therapeutic developed against SARS-CoV infection[24]. ADE has been showed in part to be induced mainly through engaging viruses and monocytes by anti-virus antibody binding with Fc Receptor or complement receptors on monocytes[24, 25, 26, 27, 28, 29, 30]. Recent studies show that sera from the COVID-19 patients with severe disease has higher NAb titer than sera from mild or asymptomatic patient[31]. Given the highly phylogenetic relationship between SARS-CoV and SARS-CoV-2, the risk of ADE will likely need to be mitigated for anti-SARS-CoV-2 development.

Here we report the isolation of several highly potent neutralizing MAbs against SARS-CoV-2 from human antibody transgenic mice. Given that ADE is a potential risk for antibody therapeutics against SARS-CoV-2 infection we introduced LALA mutation to potentially abrogate the effect in these neutralizing MAbs. One human MAb designated CA521^{LALA} demonstrated potent SARS-CoV-2-specific neutralization activity *in vitro* and *in vivo* and had no risk of ADE. Pharmacokinetics revealed that CA521^{LALA} is also stable in serum of mice and rhesus monkeys. Cryo–electron microscopy characterization of the SARS-CoV-2/CA521^{LALA} shows that it recognizes an epitope overlapping with angiotensin converting enzyme 2 (ACE2)-binding sites in SARS-CoV-2 receptor binding domain (RBD) in the Spike protein. Structural analysis reveals that the CA521^{LALA} can block the interaction by binding all three RBDs of one SARS CoV-2 spike simultaneously weather it was in 'up' or 'down' conformations.

Results

MAb CA521^{LALA} can block binding of SARS-CoV-2-RBD to hACE2 receptor and specifically bind the Spike protein of SARS-CoV-2

Potential SARS-CoV-2 targeting antibodies were identified by screening immunized human antibody transgenic mice by phage display (**Supplementary Fig. 1**). For this seven human antibody transgenic mice were immunized with recombinant Spike ectodomain (Cat 40589-V08B1, Sino Biological), RBD protein (Cat 40592-V05H, Sino Biological), Spike S1 protein (Cat 40591-V02H, Sino Biological) and Spike

S2 protein (Cat 40590-V08B, Sino Biological) of SARS-CoV-2, respectively. These antigens were also used as the baits for screening the phage antibody library. 60 potential clones were identified for in vitro evaluation. Given that ADE is a potential risk for antibody therapeutics against SARS-CoV-2 infection, LALA mutation was introduced into various targets to abrogated or eliminate the binding with Fc receptors or complement receptors during production of human monoclonal antibody. This phage display screen, *in vitro* evaluation and mutagenesis identified an excellent candidate in the novel human anti-Spike antibody CA521^{LALA} (**Supplementary Fig. 1)**.

Further analysis demonstrated that CA521 ^{LALA} blocked the binding of SARS-CoV-2-RBD with recombinant hACE2 receptor strongly compared to hACE2 protein, with IC50 as 0.343 nM, 8.887 nM respectively (**Fig. 1a**). CA521^{LALA} also showed the ability to block the binding of recombinant ACE2 to SARS-CoV-2 Spike expressing 293F cells and the binding of SARS-CoV-2 RBD to ACE2 expressing 293T cells (**Supplementary Fig. 2**). Flow cytometry (FACS) experiments revealed that CA521^{LALA} could also specifically bind to SARS-CoV-2 Spike protein transfected CHO-K1 cells (**Fig. 1b**). CA521^{LALA} could bind SARS-CoV-2-Spike specifically and not cross-react with SARS-CoV and MERS-CoV Spike (**Fig. 1c-e**). Biolayer Interferometry (BLI) using the Octet RED96 system (FortéBio) assessed the binding kinetics of CA521^{LALA}. The measured equilibrium constant (KD) of CA521^{LALA} with SARS-CoV-2-RBD, S1 and spike trimer (Shuimu BioSciences Ltd.) were 0.698 ± 0.028 nM, 6.508 ± 0.655nM and 1pM (below detection limit), respectively (**Fig. 1f-h**).

CA521 ^{LALA} shows modified binding affinity to various Fc or complement receptors in BIAcore or cell based assay

As mentioned previously, ADE is a potential risk for neutralizing MAbs agninst SARS-CoV infection. (19,20). The LALA mutation was introduced to CA521 potentially abrogates the binding with Fc receptors or complement receptors. To confirm the result of the mutation, the binding affinity of CA521^{LALA} and CA521(IgG1) to various human Fc or complement receptors were examined by Surface Plasmon Resonance (SPR) or Elisa assay. The binding affinity of CA521^{LALA} with Gama Fc Receptor 1 (CD64) was below the detection limit and in the case of FcγRIIA R167 and FcγRIIB/C it was >20 μM (**Fig. 2a-f**). Affinity of CA521^{LALA} to C1q was also significantly reduced compared with CA521(IgG1) and slightly reduced compared with Opdivo (IgG4) (**Supplementary Fig. 3**).

To further confirm abrogated binding in cell based assay, Antibody-Dependent Cellular Phagocytosis (ADCP) was conducted with SARS-CoV-2 Spike protein transfected CHO-K1 cells as target cells and macrophages derived from CD14^{+} monocytes as effector cells. Target cells were stained with CFSE and macrophages were stained with APC-anti-CD206. Double stained macrophages were considered to be macrophages that have phagocytized target cells. Phagocytosis rate of CA521^{LALA} was similar to the isotype control and lower than that of CA521(IgG1), as 3.33%, 3.76% and 12.74% respectively (**Fig. 2g-i**). For CA521^{LALA}, phagocytosis by macrophages was almost completely avoided consistent with the notation that the binding of CA521^{LALA} with Fc receptors was almost abrogated.

CA521^{LALA} inhibited SARS-CoV-2 infection *in vitro* and *in vivo*

The *in vitro* neutralization abilities of CA521^{LALA} against SARS-CoV-2 infection was evaluated using a pseudoviruses system expressing Spike protein of SARS-CoV-2 and plaque-reduction neutralization test (PRNT) against an authentic SARS-CoV-2 infection of Vero cells.

CA521^{LALA} can inhibit pseudoviruses transduction into Huh-7 and hACE2 expressing HEK293T cells with IC50 at 0.121 nM and 0.104 nM, respectively (**Fig. 3a, b**). Additionally, CA521^{LALA} also exhibited strong neutralizing activity against an authentic SARS-CoV-2 strain with a PRNT50 of 0.73 nM (**Fig. 3c**).

Next, we sought to assess the correlation between *in vitro* neutralization and *in vivo* protection. To evaluate the protection efficacy of CA521^{LALA}, BALB/c mice received MAScp6 challenge were administered intraperitoneally with a single dose of 20 mg/kg of CA521 ^{LALA} (n=4) or PBS (n=6) in a therapeutic setting (**Fig. 3d-g**). As expected, high level of viral RNAs was detected in lung and trachea at 3 days post infection in mice received PBS treatment (**Fig. 3d-e**). Remarkably, a single dose administration of CA521^{LALA} dramatically reduced RNA viral loads (**Fig. 3d, e**). CA521^{LALA} treatment resulted in a 34914-fold and 693-fold reduction of viral titers in the lungs and tracheas at 3 dpi, respectively (**Fig. 3d, e**). Histopathological examination revealed interstitial pneumonia, characterized by inflammatory cell infiltration, alveolar septal thickening and distinctive vascular system injury developed in BALB/C mice belonging to the PBS control group at 3 dpi (**Fig. 3f**). In contrast, the lungs in mice from the CA521^{LALA} treated group only showed very mild inflammatory cell infiltration, and no obvious lesions of alveolar epithelial cells or focal hemorrhage (**Fig. 3g**). These results demonstrate that CA521^{LALA} is a potent neutralizing antibody, which is effective in conferring protection on mice against SARS-CoV-2.

CA521^{LALA} is stable and has a long half-life in mice and rhesus monkeys

The pharmacokinetics of the human antibody CA521^{LALA} was studied in mice and rhesus monkeys. To achieve this a single intravenous injection dose of CA521^{LALA} was given to C57BL/6 mice (N=4) and rhesus monkeys (N=3) at 10 mg/kg and 50 mg/kg. ELISA (enzyme-linked immunosorbent assay) was used to determine the concentration of CA521^{LALA} in serum. Following a single-dose 10 mg/kg intravascular injection in C57BL/6 mice, CA521^{LALA} showed a bi-exponential serum concentration-time profile with a short distribution phase followed by a long elimination phase, with a terminal half-life (t1/2, λz) of 9.5 ± 4 days, C_{max} of 96±5 μg/mL and $AUC_{(0\text{-}t)}$ of 647 ± 43 day*μg/mL(**Fig. 4a**). Following a single-dose 50 mg/kg intravascular injection in rhesus monkeys, CA521^{LALA} showed a bi-exponential serum concentration-time profile with a short distribution phase followed by a long elimination phase, with a terminal half-life ($t_{1/2,\lambda z}$) of 9.3 ± 5 days, C_{max} of 975 ± 110 μg/mL and $AUC_{(0\text{-}t)}$ of 5101 ± 2020 day*μg/mL (**Fig. 4b**).

Cryo-electron microscopy analysis of the SARS-CoV-2 Spike protein-CA521^{LALA} complex

To investigate the interaction between CA521^{LALA} and the SARS-CoV-2 Spike protein we determined the structure of this complex using cryo-EM. Details of sample preparation, data collection and EM analysis are in the methods and extended data(**Extended Data Table 3**). In brief, purified extracellular domain of S protein (S-ECD) was incubated with full-length CA521^{LALA} and then the mixture was applied to prepare cryo-EM grids. After 2D classification good particles were selected out (**Supplementary Fig. 4**) and then subjected to 3D classification. In the good class corresponding to 614,999 particles (**Fig. 5a**) all three RBDs of the Spike trimer are “up” with three Fabs bound asymmetrically. Particles in this class were subjected to further 3D refinement with C1 symmetry to generate the consensus map of the complex. The consensus map at lower threshold showed that the two Fabs bound to RBD-1 and RBD-2 connected with each other, which suggests the bivalent binding of one CA521^{LALA} IgG molecule with two RBDs (**Fig. 5b**). In the consensus map the quality of RBD region is poor, therefore focused 3D classification and refinement of RBD region were performed to improve the local resolution of RBD-Fab interface. Finally, the local resolution of RBD region was improved to near 5 Å. The improved maps show that three RBDs bound with Fabs possess different conformations (**Fig. 5c**). Besides, the 5 Å resolution allows us to deduce the binding sites of CA521^{LALA} on RBD.

The residues of RBD mediating interaction with Fab were determined by the recognizable electron cloud density of Fab on the RBD surface (**Fig. 5d**). Two patches at RBD contributed to binding with CA521^{LALA}. The first patch includes residues 483-489(VEGFNCY). The other patch includes residues 446-451 (GGNYNY) and 493-497 (QSYGF). All these residues are located in the receptor-binding motif (RBM, 438-506) that interacts directly with ACE2.

We superimposed the crystal structure of RBD-ACE2 (cyan model) with three RBDs (red density) of S-CA521^{LALA} complex. The density of all three Fabs are in clash with ACE2, so MAb CA521^{LALA} may block the interaction of SARS-Cov-2 with human ACE2 by occupying the binding site directly (**Fig. 5e**). To compare the CA521^{LALA} and ACE2-interaction residues on the SARS-CoV-2 RBDs, we mapped them to the RBD sequences (**supplementary Fig. 5**). Seven amino acid positions were shared by CA521^{LALA} and ACE2 for the interaction with RBD, including GLY 446, Tyr 449, Phe 486, Asn 487, Tyr 489, Gln 493, Gly 496. Some CA521^{LALA} interaction residues on the SARS-CoV-2 RBDs are no more than 3 amino acids away from the direct contact residues of ACE2 on RBD, such as Val 483, Cys 488, Gly 447 and Phe 497. Main H014 and CB6-interaction residues on the SARS-CoV-2 RBDs were also mapped to the RBD sequences (**Supplementary Fig. 5**). Epitope of CA521^{LALA} is significantly different from CB6 and H014.

One IgG binding with two adjacent RBDs in one Spike trimer simultaneously may contribute to the potent blocking and neutralization ability of CA521^{LALA}. Among the residues of SARS-CoV-2 RBD mediating the interaction with MAb CA521^{LALA}, mutation variants G446V, V483I, V483A have been found in nature (reported in GISAID database up to May 6, 2020), and percentage for V483A is higher than 0.1%. The other three variants of L452R, F490L, P491R whose percentage is below 0.1% are adjacent to the interaction residues of CA521-Spike. We detected whether V483A could affect the affinity between RBD

and CA521^{LALA}. Recombinant RBD proteins harboring V483A mutation and several other mutations exhibited an basically indistinguishable binding affinity to CA521^{LALA} (**Supplementary table 4**).

Discussion

There is an urgent need for therapeutic interventions to combat the COVID-19 caused by SARS-CoV-2. Neutralizing antibodies are an important tool that can effectively fight the coronavirus[1]. CA521^{LALA} is a human neutralizing antibody that can effectively inhibit pseudovirus and authentic virus infection *in vitro* by interfering with the mechanism that the virus attaches to the host cell. CA521^{LALA} shows significant therapeutic efficacy in a newly established SARS-CoV-2 susceptible mice. CA521^{LALA} treatment resulted 34914-fold and 693-fold reduction of viral titers in the lungs and trachea at 3 dpi, respectively. Histopathological examination also showed significant improvement in the lung.

CA521^{LALA} overcomes the potential risk of antibody-dependent enhancement (ADE) for antibody therapeutics against SARS-CoV-2 infection. By introducing IgG4 subtype and LALA mutation the affinity of CA521^{LALA} to Fc Receptors, C1q or phagocytosis induced by macrophages for CA521^{LALA} was modified. Furthermore, pharmacokinetic analysis performed in mice and rhesus monkeys revealed that CA521^{LALA} was very stable and had a half-life of 9.5 ± 4 days in mice and 9.3 ± 5 days in rhesus monkeys.

The 3D structure derived from 614,999 particles of SARS-2-CoV/CA521^{LALA} complex shows that all three RBDs of the Spike protein trimers are up with Fab bound asymmetrically (**Fig. 5a**). The structure of Spike trimer is similar to previous structures of SARS-2-CoV Spike trimer in which there are always some RBDs in the closed state. Recent research shows that ACE2 binding induces the transition of RBD from close to open conformation . CA521^{LALA} may use a mechanism similar to ACE2 and promote the opening of other closed RBDs to facilitate the binding of CA521^{LALA} after binding the ‘open’ RBD.

In summary, our study identifies CA521^{LALA} as an excellent neutralizing antibody against SARS-CoV-2 with three major advantages: direct competitive binding with ACE2, binding all three RBDS of one spike simultaneously and bivalent binding of one IgG. CA521^{LALA} shows promise as an effective intervention to the COVID-19 pandemic caused by SARS-CoV-2. Potent neutralizing ability, the low risk of ADE and long half-life make it an ideal candidate to move on to clinical trial.

Materials And Methods

Ethical statement

All animal experiments were complied with relevant ethical regulations regarding animal research. Pharmacokinetics study protocols in monkeys were approved by Institutional Animal Care and Use Committee(IACUC) and the Approval Number is IACUC-A2020131-K001-01. The animal experiments for in vivo efficacy studies were conducted in Academy of Military Medical Sciences and approved by the

Experimental Animal Committee of Laboratory Animal Center, AMMS (approval number: IACUC-DWZX-2020-001). Protocols of mice experiments for immunization and pharmacokinetics study were approved by LUYE PHARMA Animal Experimentation.

Regents, Mice, Cells and Viruses

Reagents, cell lines and viral strains used in this study are listed in **Supplementary Table 1**.

Immunization

Human antibody transgenic mice were generated by Boan biotechnology. Mice were bred and kept under specific-pathogen free conditions. Seven human antibody transgenic mice were immunized in 10-day intervals with recombinant Spike S1+S2 (Cat 40589-V08B1, Sino Biological), RBD protein (Cat 40592-V05H, Sino Biological), Spike S1 protein (Cat 40591-V02H, Sino Biological) and Spike S2 protein (Cat 40590-V08B, Sino Biological) from SARS-CoV-2 strain (Wuhan-1 strain, GenBank: MN_908947), respectively. After 3 rounds immunization and one boost, spleen cells were harvested after three days of the last boost for phage libraries construction.

Phage display library construction

RNA was extracted from spleen cells of immunized mice by Trizol method. cDNA synthesis was performed using Transcriptor First Strang cDNA Synthesis Kit. The construct of the phage library was carried out according to the method described in *Phage Display: A laboratory manual* [32] The variable regions of the heavy and light chains were obtained from the cDNA by PCR. Scfv were obtained by overlapping the variable regions of heavy and light chains by PCR, and then were digested with SfiI and ligated into plasmid pCOMB3x. The ligation products are electro transfected into *E. coli* TG1 competent cells. After adding helper phage and culturing overnight, the supernatant was precipitated with PEG8000 and NaCl. Libraries were got by resuspending the pellet.

Panning of phage libraries

Plates coated with immunogen (Spike S1+S2 or Spike S1 or Spike RBD) or streptavidin- magnetic beads loading biotin-protein were used to capture phages with interest ScFvs. After washing by PBST, captured phage was eluted and then used to infect *E.Coli* TG1. Scfvs was expressed and its binding and blocking activity was tested by ELISA. Positive hits were obtained and sequenced.

Production of human monoclonal antibody

Recombinant Vector Construction

Recombinant antibody heavy chain variable region and light chain variable region were amplified (2 × Phanta Max Master Mix, Vazyme, P515-01) using the positive clones screened from the library as the template. Overlap PCR was conducted to assemble variable region and signal peptide. Purified gene fragments were separately fused (ClonExpress II One Step Cloning Kit, Vazyme, C112-01) into the linearized pcDNA3.4 vectors with constant regions. The recombinant plasmid was prepared for production. (For recombinant human mAb production, the cDNA's encoding the CA521 mAb variable regions of the heavy and light chains were cloned into expression.)

Antibody Expression and Purification

Candidate antibodies were expressed with Expi-CHO Expression system(gibco) for 12days and the supernatant was harvested and purified by protein A resin (GE healthcare). The antibodies were further purified by Q FF (GE healthcare) and Capto S ImpAct (GE healthcare) sequentially and then changed to buffer containing 10mM $CH_3COONa \cdot 3H_2O$, 30mM NaCl, 5% sucrose, 0.03% tween-20, pH5.0/6.0.

ELISA -based receptor-binding inhibition assay

High binding ELISA plates were coated with 0.5 μg/mL recombinant soluble 2019-nCoV Spike RBD at 4^{o}C overnight, and then were blocked with 3% skim milk powder in PBST (PBS containing 0.05%Tween-20) at 37^{o}C for 1 hour, following two times washing with PBST. Serially diluted CA521 was mixed with 0.04 μg/mL (final concentration) biotinylated recombinant human ACE2 and then was incubated with coated RBD in the plates at 37^{o}C for 1 hour. After washing, the biotinylated ACE2 binding to coated RBD was detected by HRP-conjugated Strep second mAb. Inhibition rate%=(OD450 of no antibody – OD450)/ OD450 of no antibody*100%. Irrelevant mAb with the same constant region of CA521 was used as isotype. Experiments were performed in triplicate, value=Mean±standard error.

Cross-reactivity by Elisa analysis

Recombinant SARS-CoV-2 Spike S1+S2 protein (40589-V08B1, Sino Biological), SARS Spike protein (SPN-S52H5, Acro) and MERS-CoV Spike protein (40069-V08B, Sino Biological) were coated on high binding ELISA plates with 0.5 μg/mL at 4^{o}C overnight. Plates were blocked with 3% skim milk powder in PBST at 37^{o}C for 1 hour and then washed two times with PBST. Serially dilutions of mAbs were added following incubation at 37^{o}C for 1 h. Plates were washed two times and then HRP-goat anti-human IgG (H+L) mAb

was used to detect antibodies binding to the Spikes. Irrelevant mAb with the same constant region of CA521 was used as isotype. Experiments were performed in triplicate, value=Mean±standard error.

Cell based binding for CA521

SARS-CoV-2 Spike protein transfected CHO cells were harvested and washed by FACS buffer (0.2% BSA in PBS) two times. 1E5 CHO-SARS-CoV-2-Spike cells were stained with isotype control IgG or CA521 at a concentration of 0.74 μg/mL at 4 ^{o}C for 1 h. After washing by FACS buffer two times, cells were incubated in dark with FITC-anti-human IgG Fc 2nd mAb at 4 ^{o}C for 30 min and then analyzed by NovoCyte 2060R flow cytometry. Irrelevant mAb with the same constant region of CA521 was used as isotype.

Experiments were performed in triplicate, value=Mean±standard error.

Affinity to SARS-CoV-2 Spike RBD mutants from different virus strain variants

The binding kinetics were assessed by Surface Plasmon Resonance (SPR) assay using the BIAcore 8K system. The measured equilibrium constant (KD) Measurements were performed at room temperature with CM5 chip, which was amino coupled by human antibody capture kit. HBS-EP+ buffer (150 mM NaCl, 10 mM HEPES, 3 mM EDTA and 0.05% (v/v) surfactant P20 pH 7.4) was used as running buffer. The blank channel of the chip served as the negative control. CA521 was captured on the chip at 400-500 response units. Serial dilutions of SARS-CoV-2-RBD mutants (from 50 nM to 3.125 nM with 2-fold dilution) were applied to flow over the chip surface which was regenerated with 3 M $MgCl_2$ after each cycle. The affinity was calculated using a 1:1 (Langmuir) binding fit model with BIAevaluation software.

Fortebio analysis of antibody binding to CoV spike antigens RBD

Antibodies to be tested were diluted to the concentration of 4 μg/mL with PBST and then immobilized onto Octet Fab2G biosensors for real-time association and dissociation. After arriving the Signal Change Threshold 1.1 nm and washed in PBST biosensor tips were immersed into the wells containing RBD protein (40592-V05H, Sino Biological) of serial dilutions and allowed to associate for 200 seconds followed by a dissociation step of 400 seconds. KD was calculated using a 1:1 binding model in Octet Data Acquisition 9.0.0.49 (Sartorius AG).

Fortebio analysis of antibody binding to CoV spike antigens Spike-Trimer

Antibodies were diluted to the concentration of 3 μg/mL with PBST and then immobilized onto ProA biosensors. After arriving at the Signal Change Threshold 0.8 nm and washing with PBST, biosensor tips were immersed into the wells containing Spike-Trimer protein of serial dilutions and allowed to associate for 200 seconds followed by a dissociation step of 400 seconds. The KD wascalculated using a 1:1 binding model in Octet Data Acquisition 9.0.0.49.

Antibody-Dependent Cellular Phagocytosis (ADCP)

Antibody-Dependent Cellular Phagocytosis (ADCP) was conducted with SARS-CoV-2 Spike protein transfected CHO-K1 cells as target cells and macrophage derived from CD14+ monocytes as effector cells. Target cells were stained with CFSE and macrophages were stained with APC-anti-CD206. Double stained macrophages are considered to have phagocytized target cells. Phagocytosis rate (in red font) = Q2-2%/(Q2-1%+Q2-2%)*100%.

ELISA-based C1q binding assay

High binding ELISA plates were coated with 100 μL 5 μg/mL CA521 subtypes at 4 °C overnight. Plates were washed four times with PBS and blocked with PBST containing 1%BSA at 37^{o}C for 1.5 hour. Fourfolds serial dilutions of mAbs starting at 40 μg/ml were added and plates were incubated for 2 hour at 37^{o}C with shaking of 180 rpm. HRP labeled anti human C1q secondary antibody diluted in 1:300 with PBST was used to detect C1q binding with mAbs.

Affinity of CA521 with different subtype to FcγRs

The binding kinetics were assessed by Surface Plasmon Resonance (SPR) assay using the BIAcore 8K system. The measured equilibrium constant (KD) Measurements were performed at room temperature with CM5 chip, which was amino coupled by His Capture Kit. HBS-EP+ buffer (150 mM NaCl, 10 mM HEPES, 3 mM EDTA and 0.05% (v/v) surfactant P20 pH 7.4) was used as running buffer. The blank channel of the chip served as the negative control. FcγRs was captured on the chip. Twofolds serial dilutions of mAbs starting at different concentration (**Supplementary Table 2**) were applied to flow over the chip surface which was regenerated with 10 mM glycine-HCl (pH 1.5) after each cycle. The affinity was calculated using a 1:1 (Langmuir) binding fit model with BIA evaluation software.

Pharmacokinetics studies of CA521^{LALA}

A single intravenous injection dose of CA521 was conducted in rhesus monkeys (N = 3, 2 females&1 male，age 3-5 years，body weight 3.00~3.90 kg) and C57BL/6 mice (N = 4, 4 males，age 5-7 weeks) at 50 mg/kg and 10 mg/kg. PK samples were collected at predose and 5 min, 30 min, 1 h, 3 h, 6 h, 24 h, 48 h, 72 h, 120 h, 168 h, 216 h, 264 h, 336 h, 504 h, 840 h, 1008 h postdose from moneys, and at predose and 3 min, 15min, 30min, 1h, 2h, 6h, 24h, 72h,120h,168h, 240h, 336h, 504h, 672h, 840, 1008h postdose. ELISA (enzyme-linked immunosorbent assay) was used to determine the concentration of $CA521^{LALA}$ in serum. In this method, SARS-CoV-2(2019-nCoV) spike protein was used as the capture reagent, and goat anti-human IgG, monkey ads-HRP was detecting agent. Results are shown as mean ± standard error (N = 3). The main PK kinetic parameters were calculated using Phoenix WinNonlin.

Neutralization assay

Pseudoviruses (80033) purchased from Beijing SanYao Science & Technology Development Company were produced and titrated as described previously [33].

SARS-CoV-2 pseudovirus were incubated with 3-fold serially diluted CA521 at 37 °C for 1 hour, and then cells suspension of Huh-7(Japanese Collection of Research Bioresources [JCRB], 0403) or HEK-293T-hACE2(CHENGDU NB BIOLAB CO., LTD) were added to the mixtures. After 24 h incubation at 37°C, neutralizations potencies of mAbs were evaluated in a luciferase assay. Luciferase activity was measured using Bio-Glo Assay reagent as a substrate (Promega). The percentage of infectivity was calculated as ratio of luciferase readout in the presence of mAbs normalized to luciferase readout in the absence of mAb. The half maximal inhibitory concentrations (IC50) were determined using 4-parameter logistic regression (GraphPad Prism). Experiments were performed in triplicate.

Infectious SARS-CoV-2 Neutralization assay

Neutralizing activity of mAbs was measured using a standard plaque reduction neutralization with Vero cells. Briefly, 5-fold serial dilutions of mAbs were added to approximately 100 PFU of SARS-CoV-2 and incubated for 1 h at 37 °C. Then, the mixture was added to Vero cell monolayers in a 24-well plate in duplicate and incubated for 1 h at 37 °C. The mixture was removed, and 1 ml of 1.0% (w/v) LMP agarose (Promega) in DMEM plus 4% (v/v) FBS was layered onto the infected cells. After further incubation at 37 °C for 2 days, the wells were stained with 1% (w/v) crystal violet dissolved in 4% (v/v) formaldehyde to visualize the plaques. PRNT50 values were determined using non-linear regression analysis. All experiments were performed followed the standard operating procedures of the approved Biosafety Level-3 facility.

Infection and antibody treatment of mice

Experiments involving live SARS-CoV-2 viruses were performed in the enhanced biosafety level 3 (P3+) facilities in the Institute of Microbiology and Epidemiology, Academy of Military Medical Sciences.

Specific pathogen-free 6-8-week female Balb/C mice were lightly anesthetized with isoflurane and transduced intranasally with 2×10^3 PFU of SARS-CoV-2 mouse adaped strain (MASCp6) in 30 μl DMEM. Groups of Balb/C mice that received SARS-CoV-2 challenge were treated intraperitoneally with a single dose of 20 mg/kg of CA521 (n=4) or PBS (n=6) at 2 h post infection. The lung and trachea tissues of mice were collected at 3 dpi for virus titer and autopsy test.

Viral RNA quantitation

Viral burden in lung and trachea from mice were measured as described previously. Briefly, lung and trachea tissue homogenates were clarified by centrifugation at 6,000 rpm for 6 min and viral RNA was extracted using the QIAamp Viral RNA Mini Kit (Qiagen) according to the manufacturer's protocol. Viral burden in each tissue sample was performed by quantitative reverse transcription PCR (RT-qPCR) targeting the S gene of SARS-CoV-2. RT-qPCR was performed using One Step PrimeScript RT-PCR Kit (Takara). The determination of the detection limit was based on the lowest level at which viral RNA was detected and remained within the range of linearity of a standard curve (Ct value of 38). RT-qPCR was performed using One Step PrimeScript RT PCR Kit (Takara, Japan) with the following primers and probes: CoV-F3 (5'-TCCTGGTGATTCTTCTTCAGGT-3'); CoV-R3 (5'-TCTGAGAGAGGGTCAAGTGC-3'); and CoV-P3 (5'-AGCTGCAGCACCAG CTGTCCA-3').The 20μl reaction mixtures were set up with 2μl of RNA. Cycling conditions were as follows: 42 °C for 5 min, 95 °C for 10 s, followed by 40 cycles of 95 °C for 5s and 60 °C for 20s.

Histology and Immunostaining

Lung tissues were excised and fixed with 10% neutral buffered formaline, dehydrated and embedded in paraffin. Sections at a thickness of 4 μm were stained with hematoxylin and eosin (H & E) according to standard histological procedures. Images were captured using Olympus BX51 microscope equipped with a DP72 camera.

Declarations

Data availability

The cryo-EM maps of Spike-CA521 complex have been deposited in EMDB under accession codes EMD-30629 (the 3.8Å consensus map) and EMD-30628 (the 4.1Å map focused on one Fab-RBD).

Acknowledgments

We thank all colleagues from Boan biotechnology and Shandong Luye Pharmaceutical (Yantai) for their support during the study. We are grateful to Shi-qi An for her help to revise the manuscript.

Funding

Boan biotechnology sponsored the studies.

Author Contributions

CD, CFQ, and LW initiated and coordinated the project. DS designed the experiments and wrote the manuscript. Y D evaluated the neutralizing potency using authentic virus, conducted animal efficacy experiments and performed histopathology assays. WW evaluated the neutralizing potency using pseudovirus. Chuangchuang Dong does the antibody screening based phage display. ZN prepared the transgenic mice. XL performed the affinity experiments with antigen. CL performed Cryo-electron microscopy examination, collected and analyzed the data. GD and JT designed the animal studies. HX dose the blocking experiments. CS and RW performed the PK studies. Y Z performed the antibody purification. QW conducted antigen immunization. JL and YL performed cell culture for antibody expression. BS does the FcR affinity experements. ZS performed the antibody quality control. JJ performed the FACS experiments. KW constructed and sequenced the antibodies. WL developed the detection assays for PK experiments.

Ethics declarations Competing interests

The authors declare no competing interests.

References

1. Mulangu S*, et al.* A Randomized, Controlled Trial of Ebola Virus Disease Therapeutics. *N Engl J Med* **381**, 2293-2303 (2019).

2. Zhou G, Zhao Q. Perspectives on therapeutic neutralizing antibodies against the Novel Coronavirus SARS-CoV-2. *Int J Biol Sci* **16**, 1718-1723 (2020).

3. Bosch BJ, van der Zee R Fau - de Haan CAM, de Haan Ca Fau - Rottier PJM, Rottier PJ. The coronavirus spike protein is a class I virus fusion protein: structural and functional characterization of the fusion core complex. *J Virol* **16**, 12 (2003).

4. Burkard C*, et al.* Coronavirus cell entry occurs through the endo-/lysosomal pathway in a proteolysis-dependent manner. *PLoS pathogens* **10**, e1004502-e1004502 (2014).

5. Millet JK, Whittaker GR. Host cell entry of Middle East respiratory syndrome coronavirus after two-step, furin-mediated activation of the spike protein. *Proceedings of the National Academy of Sciences of the United States of America* **111**, 15214-15219 (2014).

6. Millet JK, Whittaker GR. Host cell proteases: Critical determinants of coronavirus tropism and pathogenesis. *Virus Res* **202**, 120-134 (2015).

7. Walls AC*, et al.* Cryo-electron microscopy structure of a coronavirus spike glycoprotein trimer. *Nature* **531**, 114-117 (2016).

8. Walls AC, Park YJ, Tortorici MA, Wall A, McGuire AT, Veesler D. Structure, Function, and Antigenicity of the SARS-CoV-2 Spike Glycoprotein. *Cell* **181**, 281-292 e286 (2020).

9. Yuan Y*, et al.* Cryo-EM structures of MERS-CoV and SARS-CoV spike glycoproteins reveal the dynamic receptor binding domains. *Nat Commun* **8**, 15092 (2017).

10. Pallesen J*, et al.* Immunogenicity and structures of a rationally designed prefusion MERS-CoV spike antigen. *Proceedings of the National Academy of Sciences of the United States of America* **114**, E7348-E7357 (2017).

11. Gui M*, et al.* Cryo-electron microscopy structures of the SARS-CoV spike glycoprotein reveal a prerequisite conformational state for receptor binding. *Cell Res* **27**, 119-129 (2017).

12. Walls AC*, et al.* Unexpected Receptor Functional Mimicry Elucidates Activation of Coronavirus Fusion. *Cell* **176**, 1026-1039 e1015 (2019).

13. Barnes CO*, et al.* Structures of Human Antibodies Bound to SARS-CoV-2 Spike Reveal Common Epitopes and Recurrent Features of Antibodies. *Cell* **182**, 828-842.e816 (2020).

14. Daniel Wrapp NW, Kizzmekia S Corbett , Jory A Goldsmith , Ching-Lin Hsieh , Olubukola Abiona , Barney S Graham , Jason S McLellan Cryo-EM structure of the 2019-nCoV spike in the prefusion conformation. *Science*, (2020).

15. Benton DJ*, et al.* Receptor binding and priming of the spike protein of SARS-CoV-2 for membrane fusion. *Nature*, (2020).

16. Lan J*, et al.* Structure of the SARS-CoV-2 spike receptor-binding domain bound to the ACE2 receptor. *Nature* **581**, 215-220 (2020).

17. Hwang WC*, et al.* Structural basis of neutralization by a human anti-severe acute respiratory syndrome spike protein antibody, 80R. *J Biol Chem* **281**, 34610-34616 (2006).

18. Prabakaran P*, et al.* Structure of severe acute respiratory syndrome coronavirus receptor-binding domain complexed with neutralizing antibody. *J Biol Chem* **281**, 15829-15836 (2006).

19. Tian X*, et al.* Potent binding of 2019 novel coronavirus spike protein by a SARS coronavirus-specific human monoclonal antibody. *Emerg Microbes Infect* **9**, 382-385 (2020).

20. Yuan M*, et al.* A highly conserved cryptic epitope in the receptor binding domains of SARS-CoV-2 and SARS-CoV. *Science (New York, NY)* **368**, 630-633 (2020).

21. Zhang L*, et al.* Antibody responses against SARS coronavirus are correlated with disease outcome of infected individuals. *J Med Virol* **78**, 1-8 (2006).

22. Monsalvo AC*, et al.* Severe pandemic 2009 H1N1 influenza disease due to pathogenic immune complexes. *Nat Med* **17**, 195-199 (2011).

23. To KKW*, et al.* High titer and avidity of nonneutralizing antibodies against influenza vaccine antigen are associated with severe influenza. *Clin Vaccine Immunol* **19**, 1012-1018 (2012).

24. Liu L*, et al.* Anti-spike IgG causes severe acute lung injury by skewing macrophage responses during acute SARS-CoV infection. *JCI Insight* **4**, e123158 (2019).

25. Cardosa MJ. DENGUE VIRUS ISOLATION BY ANTIBODY-DEPENDENT ENHANCEMENT OF INFECTIVITY IN MACROPHAGES. *The Lancet* **329**, 193-194 (1987).

26. Prohászka Z*, et al.* Two parallel routes of the complement-mediated antibody-dependent enhancement of HIV-1 infection. *AIDS* **11**, (1997).

27. Brown MG, King CA, Sherren C, Marshall JS, Anderson R. A dominant role for FcγRII in antibody-enhanced dengue virus infection of human mast cells and associated CCL5 release. *Journal of Leukocyte Biology* **80**, 1242-1250 (2006).

28. Laurence J, Saunders A, Early E, Salmon JE. Human immunodeficiency virus infection of monocytes: relationship to Fc-gamma receptors and antibody-dependent viral enhancement. *Immunology* **70**, 338-343 (1990).

29. Littaua R, Kurane I Fau - Ennis FA, Ennis FA. Human IgG Fc receptor II mediates antibody-dependent enhancement of dengue virus infection. *J Immunol* **144** (1990).

30. Gu W*, et al.* Involvement of CD16 in antibody-dependent enhancement of porcine reproductive and respiratory syndrome virus infection. *J Gen Virol* **96**, (2015).

31. Chen X*, et al.* Disease severity dictates SARS-CoV-2-specific neutralizing antibody responses in COVID-19. *Signal Transduction and Targeted Therapy* **5**, (2020).

32. By Carlos F. Barbas III TSRIDRB, The Scripps Research Institute; Jamie K. Scott, Simon Fraser University; Gregg J. Silverman, University of California, San Diego. *Phage Display: A laboratory manual*. Cold Spring Harbor Laboratory Press (2001).

33. Nie J*, et al.* Establishment and validation of a pseudovirus neutralization assay for SARS-CoV-2. *Emerg Microbes Infect* **9**, 680-686 (2020).

Figures

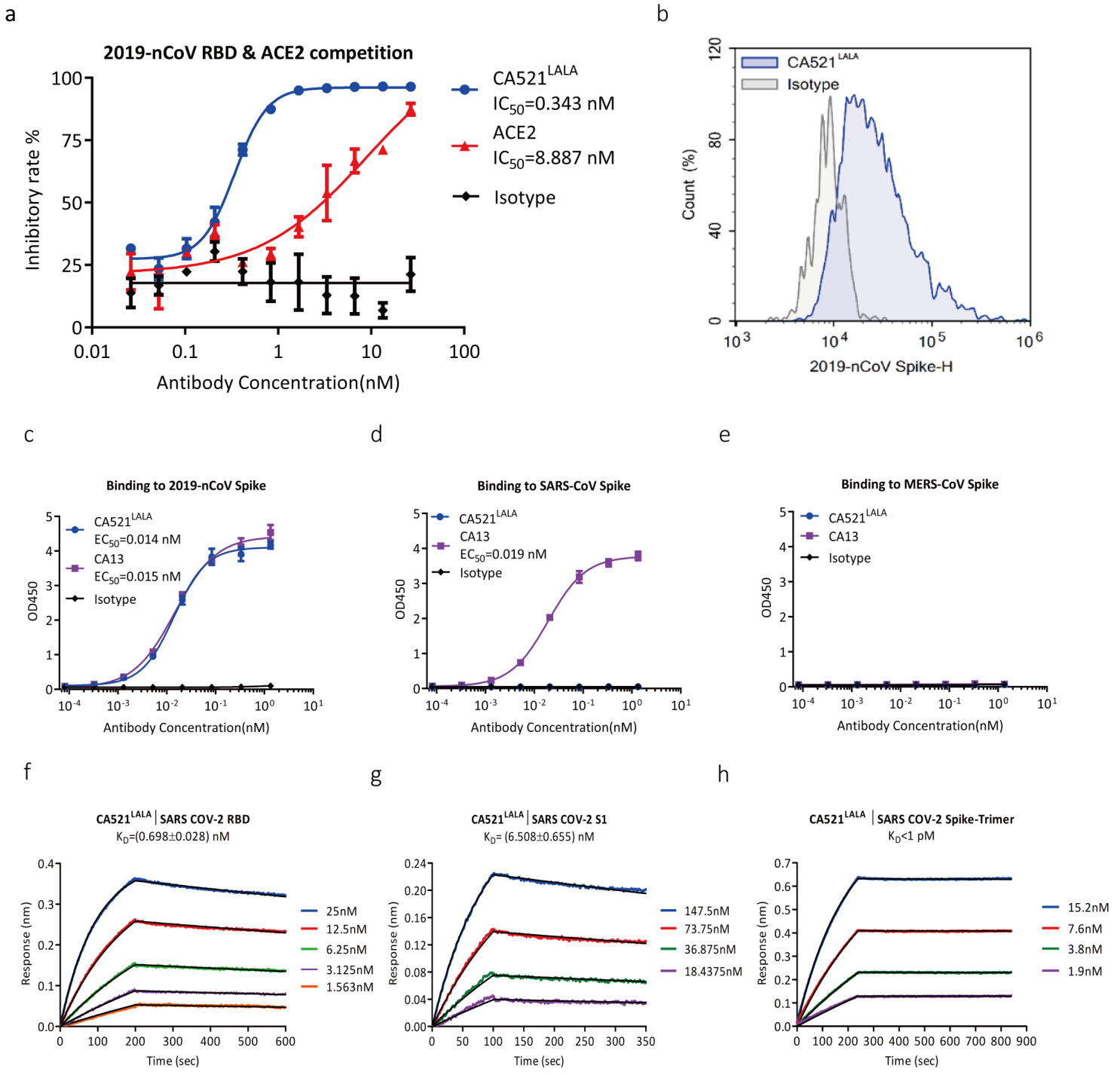

Figure 1

CA521LALA can block the binding of SARS-CoV-2-RBD to hACE2 receptor and specifically bind Spike of SARS-CoV-2 a CA521LALA can effectively block RBD binding to ACE2 receptor in ELISA. CA521LALA and hACE2 protein can block the binding of SARS-CoV-2 RBD and hACE2 with IC50 of 0.343 nM, 8.887 nM respectively. Experiments were performed in duplicate, value = Mean ± SD. b CA521LALA could specifically bind to CHO-K1 cells expressing SARS-CoV-2 Spike. SARS-CoV-2 Spike protein transfected CHO-K1 cells were stained with isotype control, CA521LALA at a concentration of 0.74 μg/mL. FITC-anti-HuFc secondary antibody was used for flow cytometry. Irrelevant mAb with the same constant region of

CA521LALA was used as isotype. Experiments were performed two times and one representative data was displayed. c-e CA521LALA could specifically bind to SARS-CoV-2 Spike protein, but does not cross-react with SARS-CoV Spike or MERS-CoV Spike protein in Elisa. CA521LALA binds SARS-CoV-2 Spike protein with EC50 of 0.014 nM. CA13, which is an anti- SARS-CoV-2 S2 domain mAb, can bind Spike of SARS-CoV-2 and SARS-CoV with EC50 of 0.015 nM and 0.019 nM. Experiments were performed in triplicate, value = Mean ± SD. f-h The binding kinetics of CA521LALA were assessed by biolayer Interferometry (BLI) assay using the Octet RED96 system (FortéBio). Trimer protein is from Shuimu BioSciences. Experiments were performed three times and one representative data was displayed.

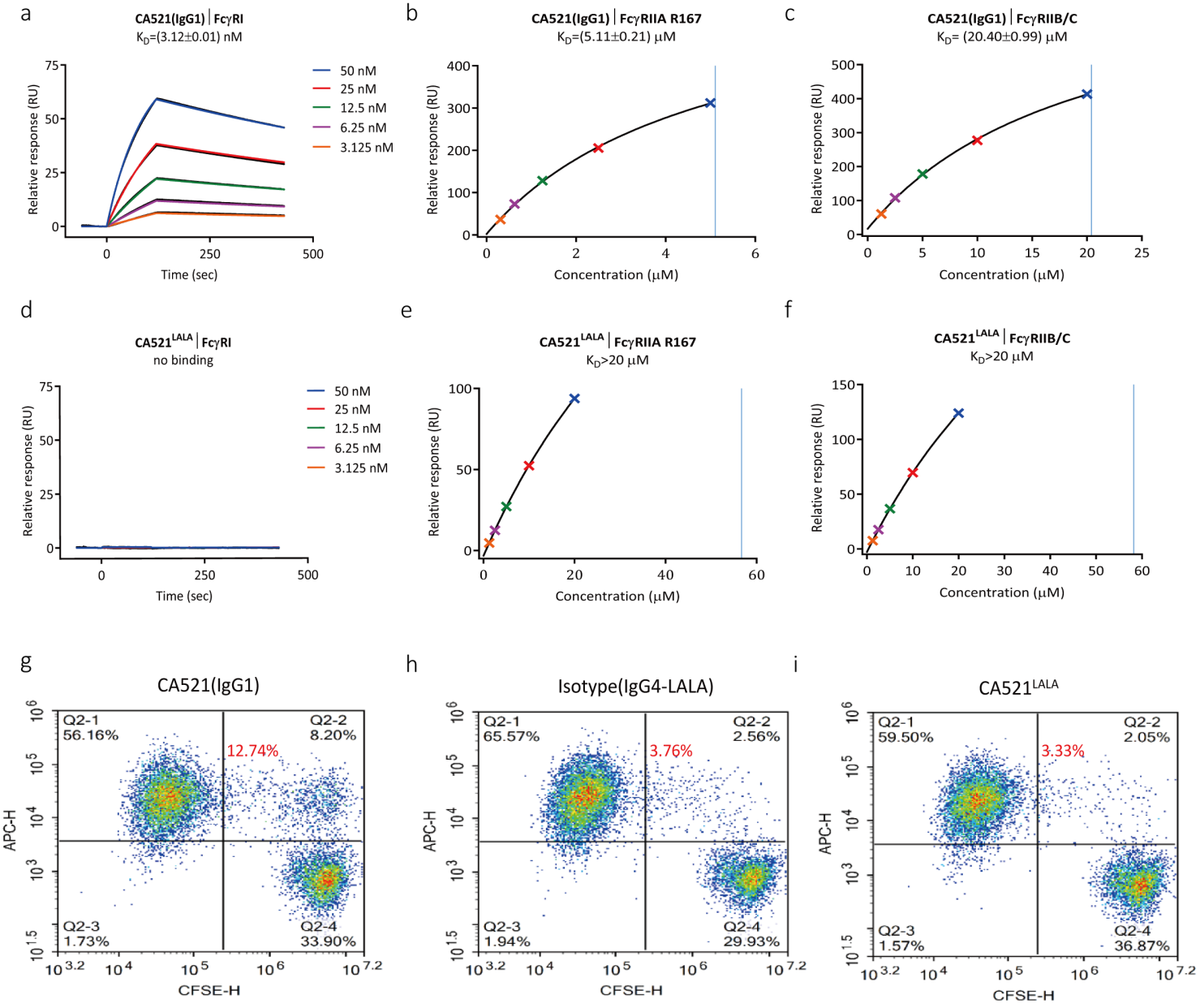

Figure 2

CA521LALA shows modified affinity to various Fc or complement receptors a-f Affinity of CA521(IgG1) and CA521LALA to FcγRI, FcγRIIA R167 and FcγRIIB/C. It was assessed by the surface plasmon resonance (SPR) assay using the BIAcore 8k system. Experiments were performed three times and one

representative data were displayed. g-i, ADCP analysis of CA521 LALA. Target cells were stained with CFSE and macrophages were stained with APC-anti-CD206. Double stained macrophages are considered to have phagocytized target cells. Phagocytosis rate (in red font) = Q2-2%/(Q2-1%+Q2-2%)*100%(double-stained macrophages/ APC-anti-CD206 stained macrophages). Phagocytosis rate for CA521(IgG1), isotype and CA521LALA were 12.74%, 3.76% and 3.33%, respectively. Experiments were performed two times and one representative data was displayed.

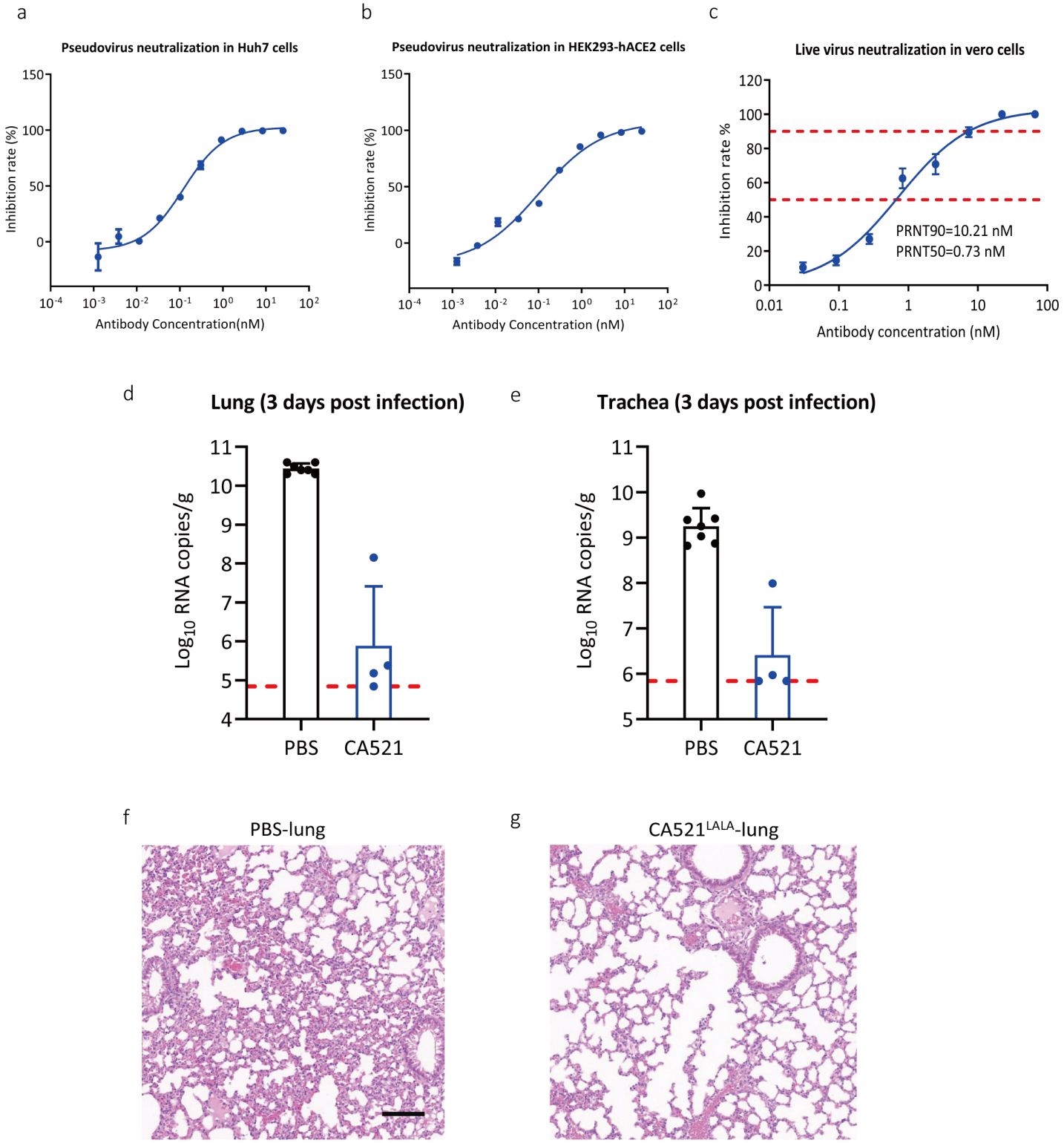

Figure 3

CA521LALA inhibited SARS-CoV-2 infection in vitro and in vivo a CA521LALA inhibits SARS-CoV-2 pseudovirus infection into Huh7 cells. b CA521LALA inhibits SARS-CoV-2 pseudovirus infection into hACE2 expressing HEK293T cells. c CA521LALA inhibit an authentic SARS-CoV-2 strain (BetaCoV/Beijing/IMEBJ01/2020) infection into Vero cells in vitro. Neutralizing activity of mAbs was measured using a standard plaque reduction neutralization with Vero cells. PRNT50 values were determined using non-linear regression analysis. d, e CA521LALA exited therapeutic efficacy in SARS-CoV-2 susceptible mice. BALB/c mice received a SARS-CoV-2 mouse adapted strain (MASCp6) challenge were administered intraperitoneally with a single dose of 20 mg/kg of CA521 LALA (n=4) or PBS (n=6) in a therapeutic setting. The level of viral RNA was detected in lung (d) and trachea (e) at 3 days post infection (3dpi) with a Quantitative PCR assay. f, g Histopathological analysis of lung samples from PBS group or CA521 LALA group at 3 dpi. Scale bar: 100 μm.

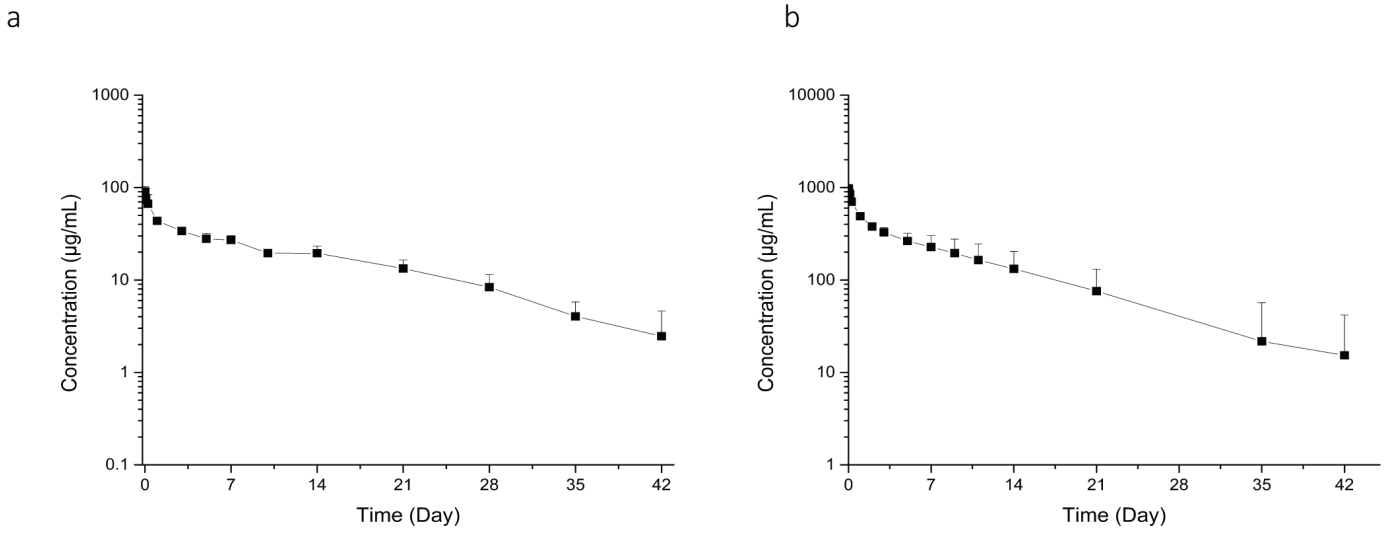

Figure 4

Log-linear serum concentration versus time profiles of CA521LALA in mice and rhesus monkeys a Four mice were administered intravenously at a dose of 10mg/kg with CA521LALA. Antibody concentrations in serum were determined in Elisa with SARS-CoV-2 (2019-nCoV) spike protein as the capture reagent. Results are shown as mean ± standard error (N = 4). b Three healthy rhesus monkeys were administered intravenously at a dose of 50mg/kg with CA521LALA. Antibody concentration in serum at different time points were determined in Elisa with SARS-CoV-2 (2019-nCoV) spike protein as the capture reagent. Results are shown as mean ± standard error (N = 3). The main PK kinetic parameters were calculated using Phoenix WinNonlin.

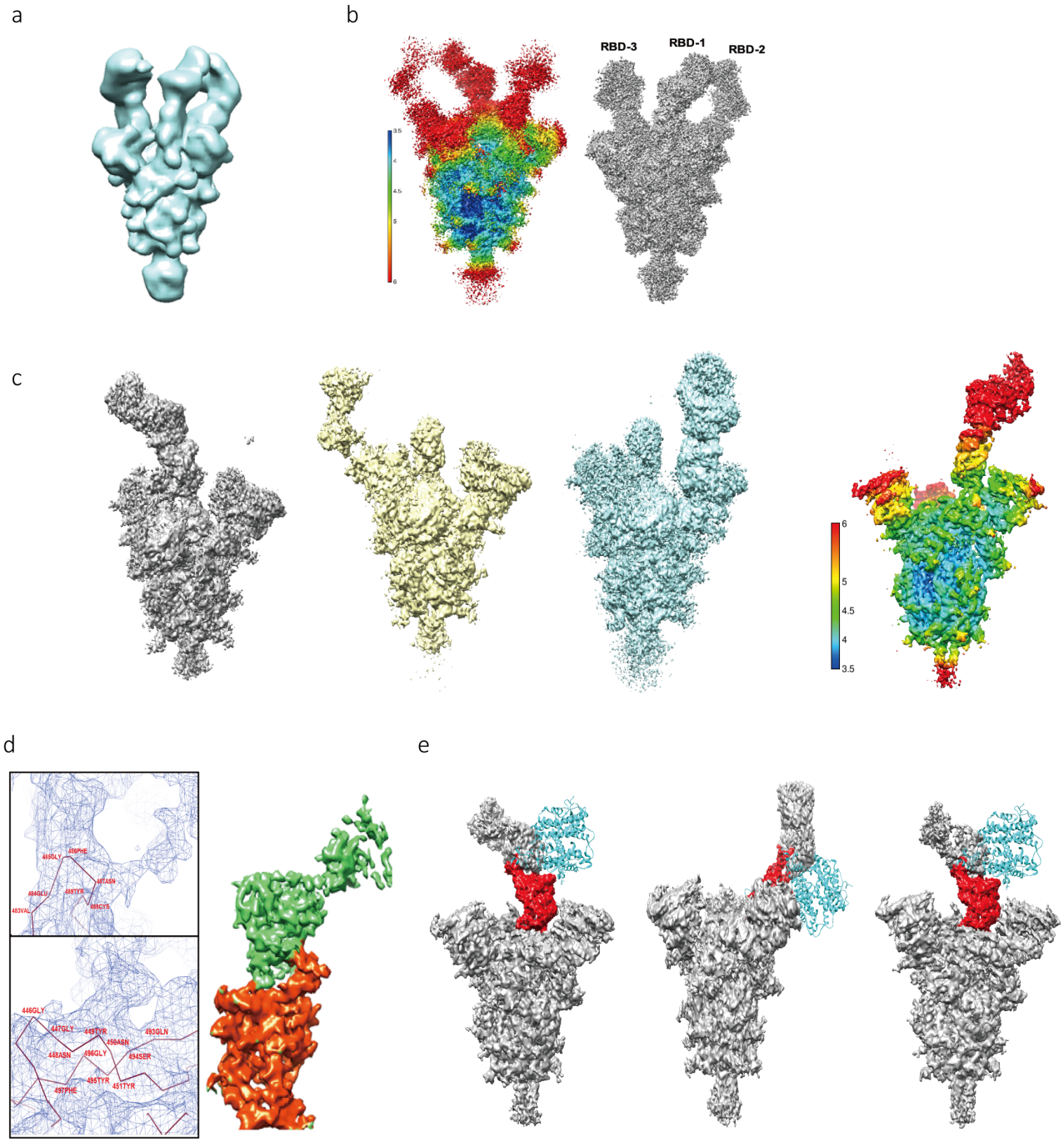

Figure 5

Three Fabs bound to three RBDs of one Spike trimer simultaneouslyand residues of RBD mediating the interaction with CA521LALA are showed. a The good class in 3D classification of intact S-CA521LALA complex. This class contains 614,999 particles. b Local resolution of the consensus map of S-CA521LALA complex (Left) and the consensus map at lower threshold (Right) to show the full density of all three RBDs. c 3D refinement focused on three RBD-Fab subcomplexes respectively (Left) and local

resolution of one of these reconstructions (Right). d The interface of RBD- CA521LALA (Left) and the whole density map of RBD-Fab subcomplex (Right). The density of RBD and Fab are displayed as blue mesh in Left panel, and in the Right panel RBD is colored with Red while Fab is colored with green. Because of the relative low resolution of RBD region, only the main chain trace (brown) of RBD is shown, and the residues mediating interaction with Fab are labeled with red color. The model of RBD is adapted from 7BWJ (PDB). e Superimposition of crystal structure of RBD-ACE2 (PDB: 6M0J, cyan model) with three RBDs (red density) of S-CA521 LALA complex. The density of all three Fabs are in clash with ACE2, so CA521 LALA may block the interaction of SARS-Cov-2 with human ACE2 by occupying the binding site.

Supplementary Files

This is a list of supplementary files associated with this preprint. Click to download.

- 1Supplementaryinformation20201029.docx